frontiers in Materials

ORIGINAL RESEARCH
published: 25 March 2022
doi: 10.3389/fmats.2022.827333

In-Situ Study of Microstructure Evolution of Spinodal Decomposition in an Al-Rich High-Entropy Alloy

*Cameron S. Jorgensen[1], Louis J. Santodonato[1,2], Kenneth C. Littrell[3], Chih Hsiang Kuo[1], Chanho Lee[1], Raymond R. Unocic[4], Peter K. Liaw[1], Dustin A. Gilbert[1,5] and Lisa M. DeBeer-Schmitt[2]**

[1]Department of Materials Sciences and Engineering, The University of Tennessee, Knoxville, TN, United States, [2]Neutron Scattering Division, Oak Ridge National Laboratory, Oak Ridge, TN, United States, [3]Neutron Technology Division, Oak Ridge National Laboratory, Oak Ridge, TN, United States, [4]Center for Nanophase Materials Sciences, Oak Ridge National Laboratory, Oak Ridge, TN, United States, [5]Department of Physics and Astronomy, University of Tennessee, Knoxville, TN, United States

High-entropy alloys (HEAs) are materials which leverage the entropy of mixing to motivate the formation of single-phase solid solutions, even of immiscible elements. While these materials are well-recognized for their application to structural engineering, there is increasing interest in the use of HEAs for functional applications such as memory storage and energy devices. The current work investigates the HEA $Al_{1.3}CoCrCuFeNi$, which has been previously shown to be single-phase at high temperatures, but undergoes phase separation at lower temperatures, transforming the structural and the functional properties. This phase separation is investigated at high temperatures with *in-situ* small angle neutron scattering (SANS) and scanning transmission electron microscopy (EDS). These techniques show that increasing the temperature up to 800°C, the microstructure of the HEA adiabatically disorders and abruptly homogenizes near 700°C, which is consistent with spinodal decomposition. Overall, the microstructural evolution proceeds mainly by the atomistic redistribution of the constituent elements within simple crystal lattices, producing coherent phase mixtures.

Keywords: high-entropy alloy (HEA), *in situ*, spinodal decomposition, microstructure, SANS (small-angle neutron scattering)

Edited by:
Dongchan Jang,
Korea Advanced Institute of Science and Technology, South Korea

Reviewed by:
Venkata Sai Kiran Chakravadhanula, Skyroot Aerospace Private Limited, India
Songqin Xia,
North China Electric Power University, China

****Correspondence:***
Lisa M. DeBeer-Schmitt
debeerschmlm@ornl.gov

Specialty section:
This article was submitted to Mechanics of Materials, a section of the journal Frontiers in Materials

Received: *01 December 2021*
Accepted: *01 March 2022*
Published: *25 March 2022*

Citation:
Jorgensen CS, Santodonato LJ, Littrell KC, Kuo CH, Lee C, Unocic RR, Liaw PK, Gilbert DA and DeBeer-Schmitt LM (2022) In-Situ Study of Microstructure Evolution of Spinodal Decomposition in an Al-Rich High-Entropy Alloy. Front. Mater. 9:827333. doi: 10.3389/fmats.2022.827333

INTRODUCTION

High-entropy alloys (HEAs) have been the focus of research since their discovery in 2004 due to their potential in structural applications (Tong et al., 2005a) and more recently functional devices such as memory storage and energy technologies (Wang et al., 2021). These materials are comprised of five or more elements which randomly occupy a single lattice site in an otherwise ordered crystal lattice; the large entropy from the chemical disorder can stabilize alloy compositions even between immiscible elements. The $Al_xCoCrCuFeNi$ family of HEAs was among the first to be studied, and continues to provide challenges and opportunities for researchers seeking to better understand phase stability, phase separation, and microstructure development in advanced alloys (Yeh et al., 2004; Tong et al., 2005b; Zhang et al., 2014; Santodonato et al., 2015; Gao et al., 2016; Miracle and Senkov, 2017; Xu et al., 2018; Pan et al., 2021). HEAs were initially recognized for their tendency to form single-phase solid solutions (e.g., alloys) with excellent mechanical properties such as high yield strength and hardness, which can be systematically varied by changing the aluminum content

(*x*-parameter) (Yeh et al., 2004; Tong et al., 2005b). Subsequent studies, particularly by Yeh et al. (2004) and Tong et al. (2005b), have revealed more details about this system, including phase separation between the Al-Ni and Cr-Fe for compositions with precentages Al ≥ 1. Commensurate with the phase separation is an enhancement of the hardness and ductility (Wang et al., 2009; Singh et al., 2011; Tang et al., 2015). The interface between these phases has been proposed to be coherent, a feature which strongly contributes to the improved structural performance in modern superalloys (Zhao et al., 2003; Prasher et al., 2019). In both the $x = 1$ and $x = 1.3$ compositions, phase separation of Al-Ni and Cr-Fe is reported at room temperature, while at high-temperatures the material is a single homogenized phase. The dissolution of the two phases has been proposed to occur by spinodal decomposition (Welk et al., 2013; Santodonato et al., 2015). The high-temperature transformation is determined by the Gibbs free energy, which couples the temperature to the entropy, affirming the role of the HEA paradigm in determining the ordering.

The high-temperature, entropically-driven transformation is the focus of the current work. Our previous work has investigated the HEA $Al_{1.3}CoCrCuFeNi$ using *in-situ* diffraction while heating through the transition, capturing changes in the crystal structure (Santodonato et al., 2015), but had little sensitivity to the microstructure or chemical ordering. Using differential thermal analysis and room-temperature microscopy, it has been proposed that the transformation occurs by spinodal decomposition (SD) at ≈600°C. During the SD, the microstructure is proposed to change abruptly, with discrete, well-defined phases merging at higher temperatures into a homogenized alloy. Due to the strong dependence of the macroscopic structural properties on the microstructure and compositional disorder (homogeneity), it is critical to develop a thorough understanding of the structure before, during and after the SD. The present study uses *in-situ* heating with small-angle neutron scattering (SANS) and scanning transmission electron microscopy (STEM) with energy dispersive x-ray spectroscopy (EDS) to investigate the temperature-dependent formation and distribution of phases, confirming the SD transition in $Al_{1.3}CoCrCuFeNi$.

EXPERIMENTAL

Samples were fabricated using standard arc melting techniques as described previously (Zhao et al., 2003; Ohmura et al., 2006; Lee et al., 2018; Lee et al., 2020a; Lee et al., 2020b). The samples for *in-situ* STEM heating experiments were prepared by first sectioning the as-cast ingots into ≈5 mm cube-shaped pieces. A Hitachi NB5000 Ga^+ focused ion beam (FIB) operated at 40 kV Ga^+ was then used to extract and thin (≈100 nm) specimens, followed by a low 5 kV surface cleaning procedure. An *in-situ* micromanipulator was subsequently employed to transfer the specimen onto a MEMS fabricated heating microchip device, (Protochips, Inc. Morrisville, NC), following the protocol outlined by Duchamp et al. (2014) FIB milling is an established technique for traditional TEM specimen preparation (Giannuzzi and Stevie, 1999) and it is well known that preparation using this method results in Ga^+ implantation (Langford and Petford-Long, 2001). However, the final cleaning at 5 kV reduces the Ga defects in the final specimen (Langford et al., 2001). The *in-situ* STEM heating experiments were performed from room temperature to 800°C on a Hitachi HF-3300 STEM, operating at 300 kV, ramping the temperature at 5°C per minute then holding the temperature constant for 30 min before imaging. STEM-EDS elemental maps were acquired using a Bruker silicon drift EDS detector at 256 × 192 pixels, a pixel dwell time of 13 ms, with an overall acquisition time of 11 min. Small-angle neutron scattering studies were conducted at the High Flux Isotope Reactor (HFIR) on the General-Purpose SANS beamline (GP-SANS) (Wignall et al., 2012). This technique is sensitive to the microstructure of the material, specifically chemical phase separation and the resulting change in the nuclear scattering length density. The instrument was configured to use a neutron wavelength (λ) of 8 Å with the resolution Δλ/λ of 0.15. The sample-to-detector distance of 19.3 m was chosen to provide a q-range of 0.002 $Å^{-1}$ to 0.04 $Å^{-1}$ for observing microstructural features in the size range of 160–3,100 Å. A tube furnace exposed to atmosphere was used to control the sample temperature during the SANS measurements, up to 800°C, allowing *in-situ* measurement of the structure. The temperature was initially heated to 400°C with a ramp rate of 20°C/s and then ramped to higher temperatures by 50°C every 15 min. The SANS prepared samples were 10 mm diameter disks with a thicknesses of 1 mm.

RESULTS AND DISCUSSION

The first step of the *in-situ* STEM-EDS study was to reproduce the previously reported room-temperature microstructure of the $Al_{1.3}CoCrCuFeNi$ alloy (Santodonato et al., 2018). The as-cast metal has a dendritic microstructure, with Cu-lean dendrites and Cu-rich inter-dendrites, spanning several hundred microns in scale (not shown). Within the dendrites, a periodic microstructure consisting of Cr-Fe rich plates in a matrix of Al-Ni of is observed and shown in **Figure 1**. The Cr-Fe has a body-centered-cubic (BCC) structure, with the plate growth direction normal to the <1 0 0 > vectors (Wang et al., 2009); the Al-Ni matrix has an ordered BCC (i.e., B2) structure. These two phases have nearly equal lattice parameters of ≈2.9 Å, allowing for a coherent interface, characterized previously by Welk *et. al.* (Welk et al., 2013) The Co (not shown) is included in both the Cr-Fe and the Al-Ni phases, with a signal appearing throughout the dendrites. The Cu is shown to form its own plates that are separate from both the Cr-Fe and the Al-Ni, which have a face-centered cubic (FCC) structure (Xu et al., 2018). Most of the Cu in the sample forms FCC phases in the inter-dendritic regions (Tong et al., 2005b; Santodonato et al., 2015; Xu et al., 2018). These FCC inter-dendritic zones are stable to temperatures near the melting point of pure Cu (1,085°C). In contrast, the oriented-plate microstructure of the dendrite region undergoes significant changes between room temperature and 800°C; which is the main focus of the present *in-situ* study.

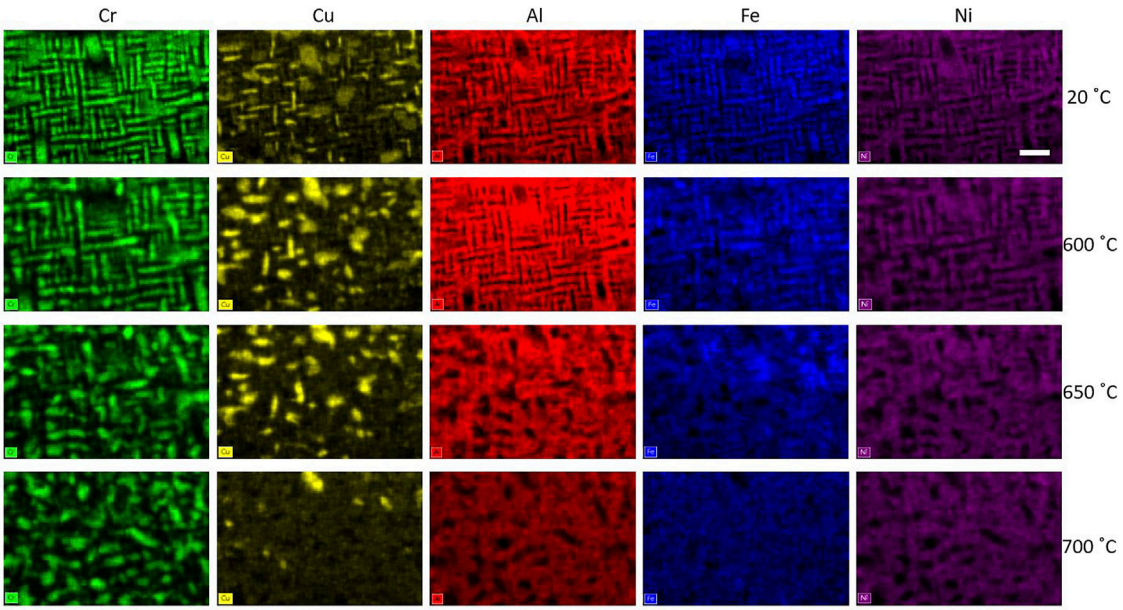

FIGURE 1 | EDS elemental maps acquired during *in-situ* STEM heating experiments of $Al_{1.3}$CoCrCuFeNi: (top to bottom) 20, 600, 650, and 700°C. Images show the compositional distributions for (left to right) Cr, Cu, Al, Fe, and Ni. Scale bar is 5,000 Å.

The STEM-EDS images in **Figure 1** show that the microstructure of the sample gradually changes as the alloy is heated from room temperature to 600°C. STEM images showing the microstructure were published in a previous work (Santodonato et al., 2015). As the Cr images emphasize, at 600°C the plates become larger, with an increasingly diffuse boundary. Increasing the temperature to 650°C further degrades the plates, causing them to lose their well-defined structure and coherent orientation. At 650°C the Fe leaves the Cr, entering the Al-Ni phase, which now forms a matrix with voids for Cr and Cu.

Finally, heating to 700°C further homogenizes the sample, resulting in a disordered dispersion of Cr-rich and Cu-rich precipitates. The Co micrograph shows that at high temperatures the Co is intermixed predominantly with the AlFeNi matrix. High-temperature neutron diffraction spectra presented in Santodonato et al. (2015) shows little change to the underlying crystal structure between room temperature and 1,000°C. Comparing the STEM-EDS results shown here to the diffraction spectra indicates that the microstructural changes occur without significant changes to the underlying crystal structures, consistent with SD.

While the STEM images show the local microstructure in the FIB-defined flake sample, a broader perspective of the bulk microstructure is necessary to confirm these results. Small angle neutron scattering is used as a bulk-technique, which is sensitive to microstructural changes in the proposed length scales but is insensitive to the crystal structure. The platelets of the different phases each have a distinct calculated neutron scattering length density: Cr (3.28×10^{-6} Å^{-2}), Cu (6.55×10^{-6} Å^{-2}), and AlFeNiCo (6.02×10^{-6} Å^{-2}). This difference enables the neutron to diffract from the plates, providing the measured signal. Furthermore, the Cu is largely segregated to the inter-dendrite boundary which is sufficiently large in scale (>1 μm) that it will not show up in the SANS data.

The SANS measurements were performed with *in-situ* heating from room temperature to 800°C using the $Al_{1.3}$CoCrCuFeNi sample, presented in **Figure 2A**. The SANS scattering patterns are plotted as a radial average of the intensity as a function of the scattering vector, Q. All of the SANS patterns show a smoothly changing, Porod-like decay. The size distribution of the microstructural phases was determined by analyzing the SANS patterns using the IRENA package (Ilavsky and Jemian, 2009). This package uses the cross-sectional scattering formula of

$$I(Q) = |\Delta\varrho|^2 \int |F(Q,r)|^2 (V(r))^2 N_p(r) dr$$

Where, $I(Q)$ is the 1D scattering intensity, $\Delta\varrho$ is the difference in scattering length density, $F(Q,r)$ is the structure factor, $V(r)$ is the volume fraction, and $N_p(r)$ is the number of particles. For the calculated analysis method, the experimental scattering pattern can be reasonably well characterized by assuming an average spherical shape, scattering length density difference and contrast for all the particles in this sample. This analysis performs a least-squares fit to determine the real-space size distribution of features within the sample. The room-temperature data shows a bimodal distribution, with a peak at ≈120 Å (**Figure 2B**), consistent with the periodicity of the platelets in the STEM images. The second, broader peak in the room-temperature curve occurs at ≈550 Å. This peak is not present in the 400°C data and is proposed to be a magnetic scattering peak as it agrees well with the expected magnetic transition below 400°C. (Huang et al., 2016) This indicates that the sample likely contains magnetic domains spanning across areas of the sample much larger than the

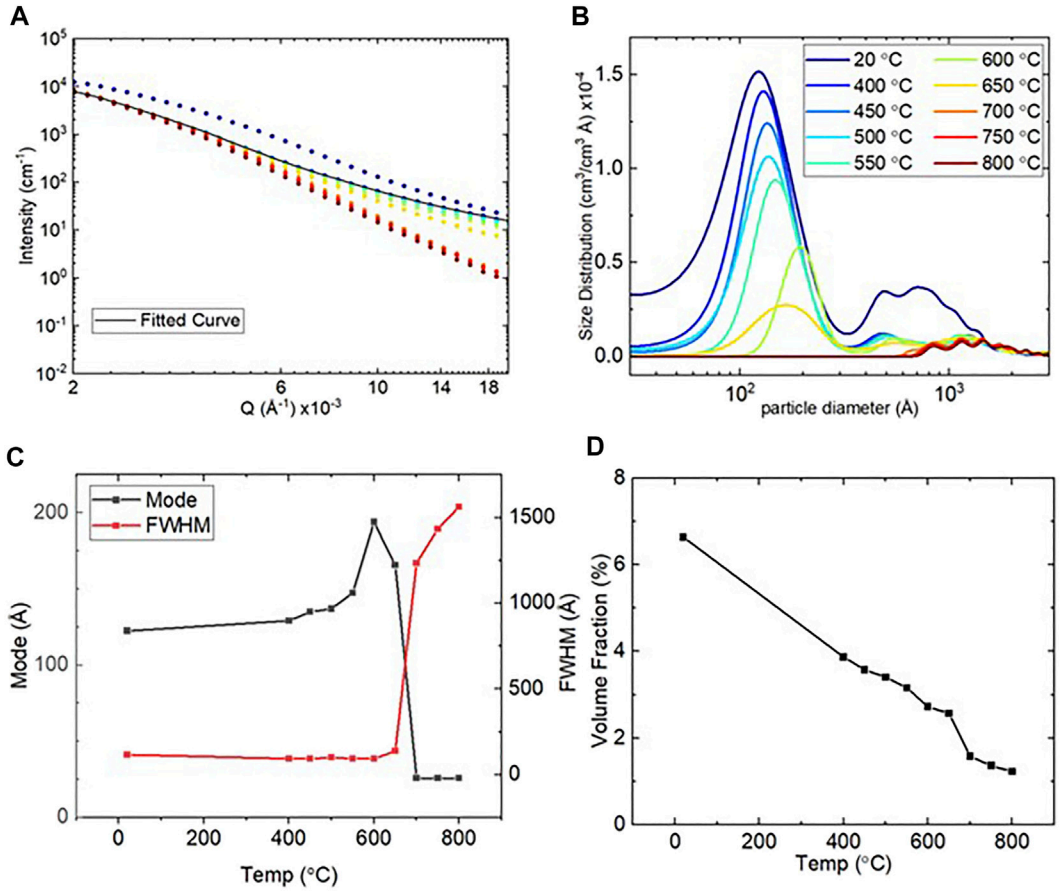

FIGURE 2 | (A) The 1D (SANS) for $Al_{1.3}$CoCrCuFeNi and the size distribution analysis. **(B)** Size distribution from the IRENA size distribution tool. **(C)** Trends in the data of the size distribution of mode and full-width at half maximum (FWHM). **(D)** Volume fraction as percentage.

platelets. Upon increasing the temperature to 600°C, the SANS data shows a continuous shift to larger diameters of the scattering centers. Accompanying this shift is a continuous decrease in the relative volume fraction (**Figure 2D**). These details are again consistent with the STEM-EDS results, which showed that the plate-like structure became larger upon approaching the SD temperature. At 600°C the STEM images also show that the boundaries of the plates are merging together as seen in the significant increase in the full-width at half-maximum of the size distribution (**Figure 2C** red curve), increasing their size beyond the range of these measurements and thus decreasing the apparent volume fraction.

As the temperature increased to the SD range, at 650°C the distribution of the scattering center sizes increases significantly in width and decreases in their average size. This trend is consistent with a reduction in the periodicity of the plate structure and the merging of the Al, Fe and Ni features seen in the STEM-EDS images in **Figure 1**. Finally, heating above 650°C, the size distribution is largely flat, indicating the loss of long-range regularity of the plate-like structures.

To summarize the combined SANS and STEM-EDS results, an expected magnetic transition is observed by SANS between 20 and 400°C due to the loss of the magnetic domain structure present at lower temperatures. Subtle changes in the microstructure occur with increasing temperatures between 400 and 600°C; these gradual changes correspond primarily to structures in the 120–200 Å range. The STEM-EDS images corroborate the growth of the nanoscale plate-like microstructure of the sample. At 650°C the STEM-EDS results show that the plates begin to lose their regularity and structure, then at 700°C the sample transforms from an ordered, quasi-oriented structure to a disordered microstructure. The sequence of gradual elemental redistribution, followed by an abrupt microstructural change, strongly suggests that a spinodal transformation occurs in $Al_{1.3}$CoCrCuFeNi, and likely in other similar alloys, as suggested in the early HEA literature (Wang et al., 2021).

CONCLUSION

The microstructure evolution of the high-entropy alloy $Al_{1.3}$CoCrCuFeNi is shown to occur by the precipitation/dissolution of ordered Fe-Cr and Al-Ni nanoplatelet phases. These chemically distinct phases have similar lattice structures and parameters, allowing for a coherent interface between them, but making it difficult to distinguish them by diffraction. The

current *in-situ* measurements (SANS and STEM-EDS) are uniquely sensitive to the chemical phase separation and were used to directly probe this phase transition. Using this sensitivity, the present work provides a direct look at the spinodal decomposition previously proposed. In addition to the SD between the Al-Ni and Fe-Cr phases, Cu-rich and Cr-rich secondary phases are observed to persist throughout the matrix at high temperatures. Throughout the transformation and homogenization process, the sample maintains a similar lattice structure and nearly constant size (Santodonato et al., 2015), implying the transformation is predominantly chemical ordering, with minimal structural contributions.

The current work, together with the previous studies (Yeh et al., 2004; Tong et al., 2005b; Santodonato et al., 2015; Zhang et al., 2016; Butler and Weaver, 2017; Xu et al., 2018), confirms that $Al_{1.3}$CoCrCuFeNi has a unique structure, consisting of a solid-solution matrix with a large fraction of secondary phases at room temperature, and up to 650°C. The secondary phases arise from both spinodal decomposition and the independent precipitation Cu-rich phases, occurring in stages at different temperatures. These phase separation processes may be used to selectively tune heat treatment for beneficial properties if properly understood and controlled. The coexistence of different formation mechanisms and the coherency of some of the resulting phases provides opportunities to explore property optimization through microstructure control. It has been noted that many important engineering alloys, such as Ni-based superalloys, owe their strength to the presence of coherent precipitates, hence similar features developed in high-entropy alloys may bring extraordinary benefits (Santodonato et al., 2015). It is in this context that the Al_xCoCrCuFeNi family of alloys should undergo further scientific and technical study, providing great opportunities for advanced alloy development.

DATA AVAILABILITY STATEMENT

The raw data supporting the conclusion of this article will be made available by the authors, without undue reservation.

AUTHOR CONTRIBUTIONS

CJ, LD-S, and DG reduced and analyzed the SANS and microscopy data. LS and PL, initiated the research concept and organized the experiments. CJ, LD-S, LS, and DG contributed to the manuscript. LS and RU conducted the *in-situ* microscopy experiments. LD-S, LS, and KL performed the SANS experiment and helped interpret the data. CK and CL fabricated the sample.

FUNDING

PL very much appreciates the supports from 1) the National Science Foundation (DMR-1611180 and 1809640) with program directors, J. Yang, G. Shiflet, and D. Farkas and 2) the US Army Research Office (W911NF-13–1-0438 and W911NF-19–2-0049) with program managers, M. P. Bakas, S. N. Mathaudhu, and D. M. Stepp.

ACKNOWLEDGMENTS

A portion of this research used resources at the High Flux Isotope Reactor, a DOE Office of Science User Facility operated by the Oak Ridge National Laboratory. The *in-situ* STEM experiments were conducted at the Center for Nanophase Materials Sciences, which is a DOE Office of Science User Facility. This manuscript has been authored by UT-Battelle, LLC under Contract No. DE-AC05-00OR22725 with the U.S. Department of Energy. The United States Government retains and the publisher, by accepting the article for publication, acknowledges that the United States Government retains a non-exclusive, paid-up, irrevocable, world-wide license to publish or reproduce the published form of this manuscript, or allow others to do so, for United States Government purposes. The Department of Energy will provide public access to these results of federally sponsored research in accordance with the DOE Public Access Plan (http://energy.gov/downloads/doe-public-access-plan).

REFERENCES

Butler, T. M., and Weaver, M. L. (2017). Investigation of the Phase Stabilities in AlNiCoCrFe High Entropy Alloys. *J. Alloys Comp.* 691, 119–129. doi:10.1016/j.jallcom.2016.08.121

Duchamp, M., Xu, Q., and Dunin-Borkowski, R. E. (2014). Convenient Preparation of High-Quality Specimens for Annealing Experiments in the Transmission Electron Microscope. *Microsc. Microanal* 20 (6), 1638–1645. doi:10.1017/S1431927614013476

Gao, M. C., Yeh, J.-W., Liaw, P. K., and Zhang, Y. (2016). *High-Entropy Alloys*. 1 edn, 1 536. Cham, Switzerland: Springer International.

Giannuzzi, L. A., and Stevie, F. A. (1999). A Review of Focused Ion Beam Milling Techniques for TEM Specimen Preparation. *Micron* 30 (3), 197–204. doi:10.1016/s0968-4328(99)00005-0

Huang, S., Li, W., Li, X., Schönecker, S., Bergqvist, L., Holmström, E., et al. (2016). Mechanism of Magnetic Transition in FeCrCoNi-Based High Entropy Alloys. *Mater. Des.* 103, 71–74. doi:10.1016/j.matdes.2016.04.053

Ilavsky, J., and Jemian, P. R. (2009). Irena: Tool Suite for Modeling and Analysis of Small-Angle Scattering. *J. Appl. Cryst.* 42, 347–353. doi:10.1107/s0021889809002222

Langford, R. M., Huang, Y. Z., Lozano-Perez, S., Titchmarsh, J. M., and Petford-Long, A. K. (2001). Preparation of Site Specific Transmission Electron Microscopy Plan-View Specimens Using a Focused Ion Beam System. *J. Vac. Sci. Technol. B* 19 (3), 755–758. doi:10.1116/1.1371317

Langford, R. M., and Petford-Long, A. K. (2001). Preparation of Transmission Electron Microscopy Cross-Section Specimens Using Focused Ion Beam Milling. *J. Vacuum Sci. Techn. A: Vacuum, Surf. Films* 19 (5), 2186–2193. doi:10.1116/1.1378072

Lee, C., Chou, Y., Kim, G., Gao, M. C., An, K., Brechtl, J., et al. (2020a). Lattice-Distortion-Enhanced Yield Strength in a Refractory High-Entropy Alloy. *Adv. Mater.* 32 (49), 2004029. doi:10.1002/adma.202004029

Lee, C., Kim, G., Chou, Y., Musicó, B. L., Gao, M. C., An, K., et al. (2020b). Temperature Dependence of Elastic and Plastic Deformation Behavior of a Refractory High-Entropy alloy. *Sci. Adv.* 6 (37), eaaz4748. doi:10.1126/sciadv.aaz4748

Lee, C., Song, G., Gao, M. C., Feng, R., Chen, P., Brechtl, J., et al. (2018). Lattice Distortion in a strong and Ductile Refractory High-Entropy alloy. *Acta Materialia* 160, 158–172. doi:10.1016/j.actamat.2018.08.053

Miracle, D. B., and Senkov, O. N. (2017). A Critical Review of High Entropy Alloys and Related Concepts. *Acta Materialia* 122, 448–511. doi:10.1016/j.actamat.2016.08.081

Ohmura, T., Tsuzaki, K., Sawada, K., and Kimura, K. (2006). Inhomogeneous Nano-Mechanical Properties in the Multi-phase Microstructure of Long-Term Aged Type 316 Stainless Steel. *J. Mater. Res.* 21 (5), 1229–1236. doi:10.1557/jmr.2006.0143

Pan, Q., Zhang, L., Feng, R., Lu, Q., An, K., Chuang, A. C., et al. (2021). Gradient Cell-Structured High-Entropy alloy with Exceptional Strength and Ductility. *Science* 374 (6570), 984–989. doi:10.1126/science.abj8114

Prasher, M., Sen, D., Bahadur, J., Tewari, R., and Krishnan, M. (2019). Correlative SANS and TEM Investigation on Precipitation Kinetics of H-phase in Ni50.3Ti29.7Hf20 High Temperature Shape Memory alloy. *J. Alloys Comp.* 779, 630–642. doi:10.1016/j.jallcom.2018.11.303

Santodonato, L. J., Liaw, P. K., Unocic, R. R., Bei, H., and Morris, J. R. (2018). Predictive Multiphase Evolution in Al-Containing High-Entropy Alloys. *Nat. Commun.* 9, 4520. doi:10.1038/s41467-018-06757-2

Santodonato, L. J., Zhang, Y., Feygenson, M., Parish, C. M., Gao, M. C., Weber, R. J. K., et al. (2015). Deviation from High-Entropy Configurations in the Atomic Distributions of a Multi-Principal-Element alloy. *Nat. Commun.* 6, 5964. doi:10.1038/ncomms6964

Singh, S., Wanderka, N., Murty, B. S., Glatzel, U., and Banhart, J. (2011). Decomposition in Multi-Component AlCoCrCuFeNi High-Entropy alloy. *Acta Materialia* 59, 182–190. doi:10.1016/j.actamat.2010.09.023

Tang, Z., Senkov, O. N., Parish, C. M., Zhang, C., Zhang, F., Santodonato, L. J., et al. (2015). Tensile Ductility of an AlCoCrFeNi Multi-phase High-Entropy alloy through Hot Isostatic Pressing (HIP) and Homogenization. *Mater. Sci. Eng. A* 647, 229–240. doi:10.1016/j.msea.2015.08.078

Tong, C.-J., Chen, M.-R., Yeh, J.-W., Lin, S.-J., Chen, S.-K., Shun, T.-T., et al. (2005a). Mechanical Performance of the Al X CoCrCuFeNi High-Entropy alloy System with Multiprincipal Elements. *Metall. Mat Trans. A.* 36 (5), 1263–1271. doi:10.1007/s11661-005-0218-9

Tong, C.-J., Chen, Y.-L., Yeh, J.-W., Lin, S.-J., Chen, S.-K., Shun, T.-T., et al. (2005b). Microstructure Characterization of Al X CoCrCuFeNi High-Entropy alloy System with Multiprincipal Elements. *Metall. Mat Trans. A.* 36, 881–893. doi:10.1007/s11661-005-0283-0

Wang, X., Guo, W., and Fu, Y. (2021). High-entropy Alloys: Emerging Materials for Advanced Functional Applications. *J. Mater. Chem. A.* 9 (2), 663–701. doi:10.1039/d0ta09601f

Wang, Y. P., Li, B. S., and Fu, H. Z. (2009). Solid Solution or Intermetallics in a High-Entropy Alloy. *Adv. Eng. Mater.* 11 (8), 641–644. doi:10.1002/adem.200900057

Welk, B. A., Williams, R. E. A., Viswanathan, G. B., Gibson, M. A., Liaw, P. K., and Fraser, H. L. (2013). Nature of the Interfaces between the Constituent Phases in the High Entropy alloy CoCrCuFeNiAl. *Ultramicroscopy* 134, 193–199. doi:10.1016/j.ultramic.2013.06.006

Wignall, G. D., Littrell, K. C., Heller, W. T., Melnichenko, Y. B., Bailey, K. M., Lynn, G. W., et al. (2012). The 40 M General Purpose Small-Angle Neutron Scattering Instrument at Oak Ridge National Laboratory. *J. Appl. Cryst.* 45, 990–998. doi:10.1107/S0021889812027057

Xu, X. D., Liu, P., Tang, Z., Hirata, A., Song, S. X., Nieh, T. G., et al. (2018). Transmission Electron Microscopy Characterization of Dislocation Structure in a Face-Centered Cubic High-Entropy alloy Al0.1CoCrFeNi. *Acta Materialia* 144, 107–115. doi:10.1016/j.actamat.2017.10.050

Yeh, J.-W., Chen, S.-K., Lin, S.-J., Gan, J.-Y., Chin, T.-S., Shun, T.-T., et al. (2004). Nanostructured High-Entropy Alloys with Multiple Principal Elements: Novel alloy Design Concepts and Outcomes. *Adv. Eng. Mater.* 6, 299–303. doi:10.1002/adem.200300567

Zhang, C., Zhang, F., Diao, H., Gao, M. C., Tang, Z., Poplawsky, J. D., et al. (2016). Understanding Phase Stability of Al-Co-Cr-Fe-Ni High Entropy Alloys. *Mater. Des.* 109, 425–433. doi:10.1016/j.matdes.2016.07.073

Zhang, Y., Zuo, T. T., Tang, Z., Gao, M. C., Dahmen, K. A., Liaw, P. K., et al. (2014). Microstructures and Properties of High-Entropy Alloys. *Prog. Mater. Sci.* 61, 1–93. doi:10.1016/j.pmatsci.2013.10.001

Zhao, S., Xie, X., Smith, G. D., and Patel, S. J. (2003). Microstructural Stability and Mechanical Properties of a New Nickel-Based Superalloy. *Mater. Sci. Eng. A* 355 (1-2), 96–105. doi:10.1016/S0921-5093(03)00051-0

Conflict of Interest: The authors declare that the research was conducted in the absence of any commercial or financial relationships that could be construed as a potential conflict of interest.